ResearchGate

See discussions, stats, and author profiles for this publication at: https://www.researchgate.net/publication/237000660

Off- Design Operation and Exergy Analysis of Multi-Stage Compressors

Article · January 2013

CITATION
1

READS
923

2 authors:

Ahmet Ozan Gezerman
Toros Agri Industry and Trade
85 PUBLICATIONS **396** CITATIONS
SEE PROFILE



Burcu didem çorbacıoğlu
Yıldız Technical University
25 PUBLICATIONS **66** CITATIONS
SEE PROFILE

All content following this page was uploaded by Ahmet Ozan Gezerman on 11 January 2014.

The user has requested enhancement of the downloaded file.

International Journal of Modern Engineering Sciences, 2013, 2(1): 39-50

Modern Scientific Press

International Journal of Modern Engineering Sciences **ISSN: 2167-1133**

Journal homepage:www.ModernScientificPress.com/Journals/IJMES.aspx *Florida, USA*

Article

Off-Design Operation and Exergy Analysis of Multi-Stage Compressors

Ahmet Ozan Gezerman*, Burcu Didem Çorbacıoğlu

Department of Chemical Engineering, Faculty of Chemical- Metallurgical, Yildiz Technical University, Istanbul, Turkey

* Author to whom correspondence should be addressed; E-Mail: ahmet_ozan@yahoo.com; Tel.: + 90 532 653 85 05; + 90 536 341 69 59

Article history: Received 9 April 2013, Received in revised form 29 May 2013, Accepted 29 May 2013, Published 30 May 2013.

Abstract: Today, multi-stage compressors serve in many industry branches. The multi-stage compressor design is primarily focused on storage or process conditions. Outside of the guaranteed time that the compressor manufacturer ensures, material fatigue and other mechanical problems that occur during process cause off-design operation of compressors. In this study, the relative Mach number in the discharge and inducer, including the non-dimensional mass flow rate are studied and compared with appropriate available theory.

Keywords: multi-stage compressor; inducer; discharge; impeller

---

1. Introduction

Horlock was the first to calculate flow parameters on turbomachine and to rearrange calculations including entropy changes [1]. Galvas showed that the maximum efficiency for an impeller inclined back can have specific speed values between 0.705 and 1.018 [2].

Whitfield and Baines presented a general design procedure for a multi-stage compressor and turbine. They described a loss coefficient for calculating enthalpy losses for real flow compared to

Copyright © 2013 by Modern Scientific Press Company, Florida, USA

ideal flow in the impeller. Further, they developed a design including losses for dimensional flow by bringing this loss coefficient to the right side of the non-dimensional mass flow parameter [3].

Toyoma et al. investigated the results of measurements conducted in a multi-stage compressor that had high pressure ratio during operation in the turbulence area. They showed how turbulence occurred in an impeller and how pressure fluctuated with turbulence [4].

Baines and Wallace presented a design procedure based on the estimation of entropy loss for off-design operation after calculating the designing point for turbodischarge applications that use a multi-stage compressor and turbine Baines and Wallace [5]. They determined appropriate operation conditions by showing motor speeds on turbine performance curves.

Koçak reported studies on calculation of preliminary design. He investigated the effect of lack of power factor on the discharge diameter. He showed the effects of inducer geometry and critical flow conditions on relative Mach number in the inducer. He presented a preliminary design procedure that uses an impeller diffuser and a diffuser that has no impeller [6].

In this study, revolutions per minute, pressure capacity, impeller dimensions depending on mass flow, and changes in relative Mach number in the inducer for off-design operation were calculated by iteration. Aerothermodynamic and aerodynamic parameters depending on the new values were calculated. These values were used to draw performance curves on a stall line that did not require a multi-stage impeller to work or on Mach number with value 1, which is in the critical flow region.

2. Determination of Impeller Dimensions

Preliminary design calculations are performed according to compressor speed, pressure capacity, and flow rate. Therefore, an impeller, which is the most important equipment in multi-stage compressor, should have appropriate dimensions.

Rodgers has described the operation factor as

$$\lambda = \frac{C_{2\theta}}{U_2} = \frac{\mu}{1-\frac{tan\beta_{B2}}{tan\alpha_2}} \quad (1)$$

where λ shows the operation input coefficient. In this paper, H is the enthalpy; r, diameter; c, the absolute velocity; W, the relative velocity; U, the impeller velocity; α, the angle of absolute velocity; β, the angle of relative velocity; 1, the subscript for the inducer; 2, the subscript for the discharge; θ, the tangential direction; ∞, the endless impeller; 1h, the subscript for the bottom side of the inducer; 1s, the subscript for the top side of the impeller; 0, the stop position; m, the meridional direction; and 2B, the subscript for the impeller angle on the endless impeller [7].

Copyright © 2013 by Modern Scientific Press Company, Florida, USA

From Figure 1, we obtain stop pressure ratios as follows.

$$\frac{P_{02s}}{P_{01}} \cong \frac{P_{02}}{P_{01}} \tag{2}$$

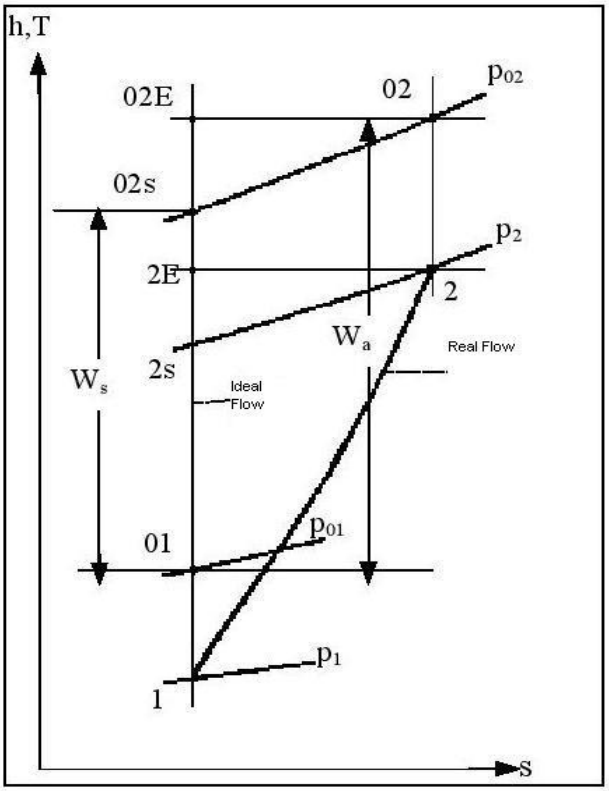


Figure 1. h-s diagram of multi- stage compressor

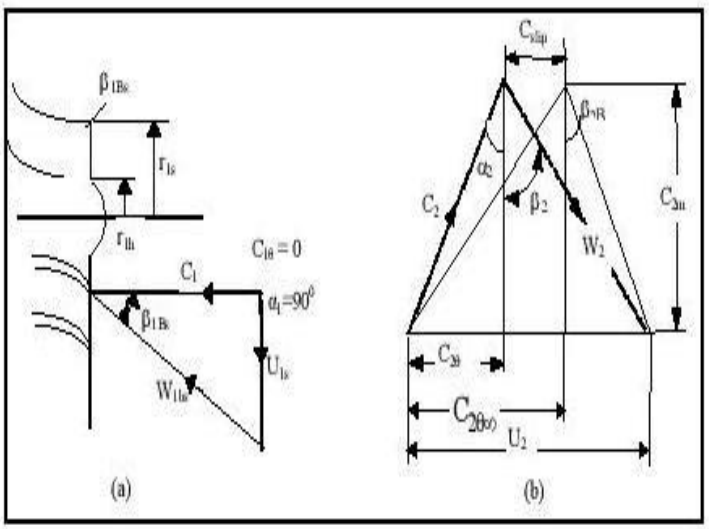


Figure 2. (a) velocity triangle of inducer, and (b) velocity triangle of discharge

Copyright © 2013 by Modern Scientific Press Company, Florida, USA

From equation (2), we obtain specific impeller operation,

$$W = h_{02} - h_{01} = U_2 C_{2\theta} - U_1 C_{1\theta} \quad (3)$$

For an ideal gas, the total efficiency, is written as shown in equation (4),

$$\eta_s = \frac{W_s}{W_a} = \frac{h_{02s} - h_{01}}{h_{02} - h_{01}} = \frac{C_p T_{01}}{U_2 C_{2\theta} - U_1 C_{1\theta}} \left(P_R^{\frac{\chi-1}{\chi}} - 1 \right) \quad (4)$$

Where Ws is the entropic work; Wa, the real work; η_s, the entropic efficiency; C_p, the specific heat under fixed pressure; and x, the ratio of specific heats (isentropic subscript).

If there is no direction on inducer input, i.e., $C_{1\theta} = 0$, and if equations (1), (2), and (3) are substituted in equation (4), we obtain

$$\frac{U_2}{a_{01}} = \frac{\left(P_R^{\frac{\chi-1}{\chi}} - 1 \right) - 1}{\eta_s \lambda (\chi - 1)} \quad (5)$$

Here, *a* is the sound velocity.

The flow coefficient is expressed as equation (6) by Whitfield and Baines [8]:

$$\Phi = \frac{\rho_1}{\rho_{01}} \left(\frac{r_{1s}}{r_2} \right)^2 (1 - v^2) \frac{C_1}{a_{01}} \frac{a_{01}}{U_2} \quad (6)$$

where r is the diameter, ρ is the density and V = $\frac{r_{1h}}{r_{1s}}$

From Figure 2(b), the meridional velocity rate of the discharge is expressed as follows:

$$\frac{C_{2m}}{a_{01}} = \frac{C_{2\theta}}{a_{01}} \frac{1}{tan \propto_2} \quad (7)$$

The density ratio of the discharge is

$$\frac{\rho_2}{\rho_{01}} = \left(\frac{p_2}{p_{01}} \right) \left(\frac{T_{02}}{T_2} \right) \left(\frac{T_{01}}{T_{02}} \right) \quad (8)$$

Copyright © 2013 by Modern Scientific Press Company, Florida, USA

and the dimension ratio of discharge [9] is

$$\frac{b_2}{r_2} = \frac{\Phi\frac{U_2}{a_{01}}}{2\frac{\rho_2\, C_{2m}}{\rho_{01}\, a_{01}}} \tag{9}$$

where b_2 is the impeller width.

3. Off-Design Operation Conditions

Pressure capacity, flow rate, non-dimensional mass flow parameter, and revolution number, which are design values or operation parameters, are given by

$$\frac{\frac{m\sqrt{RT_{bo}}}{\chi}}{Ap_{b0}} = M_b\left(1+\frac{(\chi-1)M_b^2}{2}\right)^{-\frac{(\chi+1)}{2(\chi-1)}} \tag{10}$$

as reported previously [10].

Under design conditions such as revolution number, decrease in enthalpy, and unexpected mass flow rate, off-design operation occurs.

If Equation (10) is arranged for discharge, then

$$\frac{\frac{m\sqrt{RT_{b02}}}{\chi}}{A_2 p_{b01}} = \frac{\frac{m\sqrt{RT_{b02}}}{\chi}}{A_2 p_{b01}}\left(\frac{T_{b02}}{T_{b01}}\right)^{\frac{1}{2}}\left(\frac{p_{b01}}{p_{b02}}\right) \tag{11}$$

If the flow has a β_2 angle on the discharge, equation (11) becomes

$$\frac{\frac{m\sqrt{RT_{b02}}}{\chi}}{A_1 p_{b02}} = \frac{A_2}{A_1}\cos\beta_2 M_{b2}\left(1+\frac{\chi-1}{2}M_{b2}^2\right)^{\frac{\chi+1}{2(\chi-1)}} \tag{12}$$

and can be written as the non-dimensional mass flow rate of the discharge. The second expression on the right side of equation (11) is given by

$$\frac{T_{b02}}{T_{b01}} = 1 - \frac{1}{2C_{pT_{b01}}}\left(U_1^2 - U_2^2\right) \tag{13}$$

Copyright © 2013 by Modern Scientific Press Company, Florida, USA

and is the relative stop temperature ratio. The third expression on the right side of equation (11),

$$\frac{p_{b02}}{p_{b01}} = [1 - \frac{1}{2C_p T_{b01}}(U_1^2 - U_2^2)]^{\frac{\chi}{\chi-1}} \quad (14)$$

is the ratio of the relative stop pressure, where subscript b shows relative position.

If equations (12), (13), and (14) are substituted in equation (11), the following expression is obtained:

$$\frac{m\sqrt{\frac{RT_{b01}}{\chi}}}{A_1\ p_{b01}} = \frac{A_2}{A_1} cos\beta_2 M_{b2}(1 + \frac{\chi-1}{2} M_{b2}^2)^{\frac{\chi+1}{2(\chi-1)}}[1 - \frac{\chi-1}{2\chi RT_{b01}}(U_2^2 - U_1^2)]^{\frac{\chi+1}{2(\chi-1)}} \quad (15)$$

The amount of entropy change obtained are given by

$$\int_{s_{01}}^{s_{02E}} ds = C_p \int_{T_{01}}^{T_{02E}} \frac{dT}{T} - R \int_{p_{01}}^{p_{02E}} \frac{dp}{p} \quad (16)$$

$$C_p\ ln(\frac{T_{01}}{T_{02E}}) = -Rln(\frac{p_{02E}}{p_{01}}) \quad (17)$$

Equation (16) when integrated between (01-02) processes,

$$s_{01} - s_{02} = C_p ln(\frac{T_{01}}{T_{02}}) + Rln(\frac{p_{02}}{p_{01}}) \quad (18)$$

is obtained, and if it is substituted in (17),

$$\frac{p_{02}}{p_{02E}} = e^{(-\frac{\Delta s}{R})} \quad (19)$$

where Δs is the entropy change in a real process. Furthermore,

$$\sigma = e^{(-\frac{\Delta s}{R})} \quad (20)$$

Equation (20) for the rotor is as follows [3].

Copyright © 2013 by Modern Scientific Press Company, Florida, USA

$$\sigma = \left(\frac{T_{b01}}{T_{b02}}\right)^{\frac{\chi}{\chi-1}} \left(\frac{p_{b02}}{p_{b01}}\right) \quad (21)$$

For including entropy change, equation (21) is placed on the right side of equation (15).From the ratio of the bottom and top side diameters of the inducer r_{1s}/r_{2s}, ratio of the top side diameter of the inducer and the discharges diameter r_{1h}/r_2, top side flow angle of inducer (B_{1s}), compressor stage's efficiency (η_s), lack of power factor (m), impeller angle on the discharge ($\propto_2$), the most efficient points were chosen.

In the performance of the multi-stage/multi-stage compressor, because the operation location and conditions change, calculations are made according to the stop pressure of the inducer (p_{01}), stop temperature of the inducer (T_{01}), stop pressure ratio of the compressor (PR),and the angle of the discharge inclined back.

Because inducer area A_1 and discharge area A_2 are found by design calculations, the left side of equation (11) depends on input conditions, but the right side of equation (11) depends on the relative flow angle of the discharge, relative Mach number, and revolution number.

The impeller is dimensioned according to the movement of the designed point to off-design operation conditions when the revolution number and mass flow rate change. Off-design calculations are carried out in the following order.

The left side of equation (15) is calculated. The right side of equation (16) is calculated by including the blockage factor depending on the Mach number determined in the preliminary design
The relative temperature ratio of the discharge,

$$\frac{T_{b02}}{T_2} = \left(1 + \frac{\chi-1}{2} M_{b2}^2\right) \quad (22)$$

the relative Mach number of the discharge,

$$M_{b2} = \frac{W_2}{a_2} = \frac{W_2}{\sqrt{\chi RT}} \quad (23)$$

and equation (22) are substituted in equation (23); if it is arranged depending on the relative Mach number of the discharge, then

$$W_2 = M_{b2}\left[\frac{\chi R T_{b02}}{1+\frac{\chi-1}{2}M_{b2}^2}\right]^{\frac{1}{2}} \quad (24)$$

is obtained as relative the Mach number of the discharge.

Copyright © 2013 by Modern Scientific Press Company, Florida, USA

4. Flow Angle of Discharge

The lack of power factor is [8],

$$\mu=1-\frac{C_{2\theta\infty}-C_{2\theta}}{U_2} \tag{25}$$

The tangential velocity component of absolute velocity for endless impeller position is

$$C_{2\theta\infty}=U_2+W_{2\theta\infty}=U_2+W_2 sin\beta_{B2} \tag{26}$$

Equation (26) depending on the meridional velocity component becomes

$$C_{2\theta\infty}=U_2+C_{2m}\,tan\beta_{B2} \tag{27}$$

The tangential component of absolute velocity from a real velocity triangle shown in Figure 2(b) is obtained as

$$C_{2\theta}=U_2+C_{2m}tan\beta_2 \tag{28}$$

If equation (26) is substituted in equation (25),

$$C_{2\theta}=\mu U_2+C_{2m}tan\beta_{B2} \tag{29}$$

is obtained. If equation (29) is equalized to equation (30),

$$\frac{U_2}{W_2}(1-\mu)=cos\beta_2 tan\beta_{B2}-sin\beta_2 \tag{30}$$

is obtained.

If equation (30) is arranged on a real flow triangle depending on the relative velocity angle,

$$sin\beta_2=\frac{\frac{U_2}{W_2}(1-\mu)+tan\beta_{B2}[1+tan^2\beta_{B2}-\frac{U_2^2(1-\mu)^2}{W_2^2}]^{\frac{1}{2}}}{1+tan^2\beta_{B2}} \tag{31}$$

Copyright © 2013 by Modern Scientific Press Company, Florida, USA

is obtained. Thus, the relative velocity angle on discharge is found.

The right side of equation (15) is determined from the Mach number obtained by iteration and angle obtained from equation (31). The relative Mach number is iterated until the right side of equation (15) equals the left side. The relative Mach number obtained is the Mach number that depends on the preliminary design flow. For off-design operation conditions, U_1 and U_2 values are found. Because the impeller is dimensioned and B_{1s} and α_2 are known, C_1 and W_{1s} values are calculated from the inducer velocity triangle. Because T_{01} and P_{01} are known, T_1, T_{b01}, T_{b02} are calculated from the adiabatic energy equation, the isentropic process equation, and p1, respectively. The non-dimensional mass flow parameter at the left side of equation (15) is found. For the right side of equation (15), iteration begins with the relative Mach number obtained at the design point.

The relative Mach number is calculated using equation (19).The discharge flow angle is calculated using equation (31). The right side of equation (15) is calculated using the relative Mach number obtained by iteration and the angle obtained using equation (31). The relative Mach number is iterated until the right side of equation (15) equals the left side. The relative Mach number obtained is the Mach number for off-design flow. T_2, p_2, T_{02}, p_{02}, and p_{b02} are obtained using trigonometric relationships from the discharge velocity triangle, C_2, W_2, (h-s) diagram, and thermodynamic relationships.

5. Results and Discussion

Compressors designed for use in industry should be able to operate seamlessly under all process conditions. Use of a multi-stage compressor is one of the most appropriate alternatives. Multi-stage compressors can ensure a higher pressure ratio than single stage compressors and a higher flow rate than screw compressors, with lower manufacturing and maintenance costs. They can work more efficiently and reliably under all operation conditions.

Multi-stage compressors consist of three parts. An inducer, through which gas enters, an impeller, wherein the kinetic energy of the gas is increased, and a diffuser (discharge), wherein kinetic energy is converted to potential energy. In multi-stage systems, the inlet part is designed depending on the outlet part. If cooling is required for this system, the cooling system is inserted between the outlet and the inlet. In single stage systems, there is a collection chamber after the diffuser, which ensures that gas moves in the required direction.

Although impeller design, which ensures energy transfer in a multi-stage compressor, is dimensioned depending on the preliminary design, a multi-stage compressor impeller does not always operate at designed points in an aircraft engine or in the filling system of internal combustion engines. As seen in Öztürk's compressor curves [11], if the fixed revolution number decreases, pressure ratio

Copyright © 2013 by Modern Scientific Press Company, Florida, USA

increases. However, after the mass flow rate determined, the boundary layer, called the rotating stall, begins to separate from the surface of the impeller. This unstable region is due to the vibration of the exposed multi-stage compressor and material fatigue. The impeller of the multi-stage compressor operates under the conditions between the minimum mass flow rate with which the rotating stall begins to rotate and the critical flow conditions under which the Mach number is 1. Under these conditions, off-design operation conditions of the compressor occur.

In the case of off-design operation, aerodynamic and aerothermodynamic parameter changes occur in the inducer; therefore, aerodynamic and aerothermodynamic parameter changes occur for the discharge, as well. Therefore, the stop pressure (p_{02}/p_{01}) and the stop temperature ratio (T_{02}/T_{01}) are changed according to the ideal flow shown in Figures 3 and 4. When the curves in the figures, obtained from the study conducted by Whitfield and Baines [8], are drawn according to (U_2/a_{01}) values, in the operation region border, as can be seen in Braembussche's study in 1990, the accuracy of the off-design operation procedure can be observed.

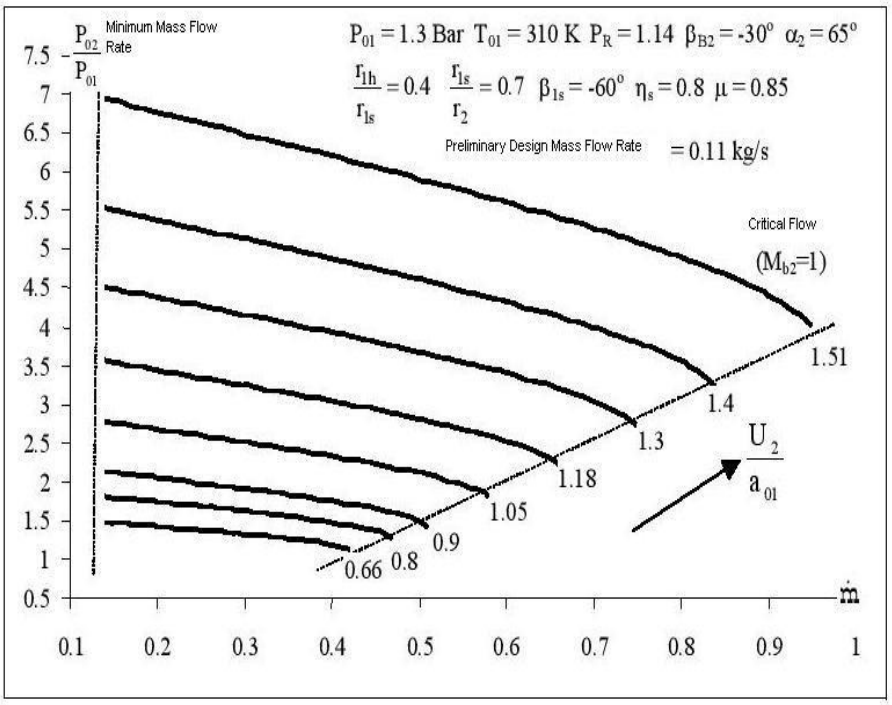


Figure 3. Changes in performance parameters depending on stop pressure ratio under ideal flow conditions.

Copyright © 2013 by Modern Scientific Press Company, Florida, USA

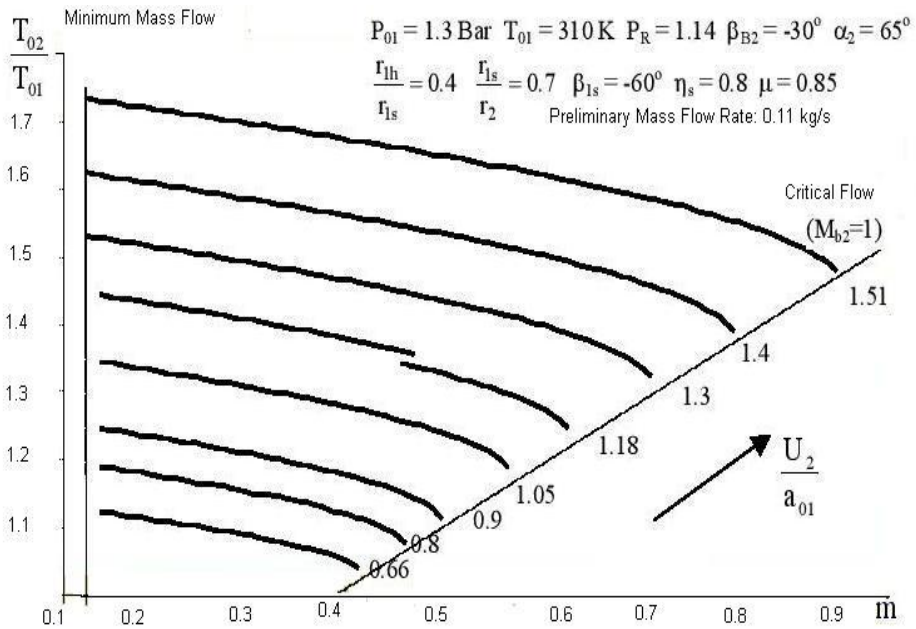


Figure 4. Changes performance parameters depending on stop temperature ratio under ideal flow conditions

The 5% difference in numerical values is derived from constant values in calculation of off-design operation. This constant is the value of enthalpy losses obtained in the preliminary design. This deviation is within acceptable limits.

References

[1] Horlock, J. H., On Entropy Production in Adiabatic Flow in Turbomachines, ASME, *Journal of Basic Engineering*, 93(**1971**): 587-593.

[2] Galvas, M. R., Analytical Correlation of Multi-stage Compressor Design Geometry for Maximum Efficiency with Specific Speed, *NASA TN D*, 6729(**1972**): 39.

[3] Whitfield, A. and Baines, N. C. A., General Computer Solution for Radial and Mixed Flow Turbomachines Performance Prediction, *Int. J. Mech. Sci.*, 18(**1976**): 179-184.

[4] Toyoma, K.; Runstadler, P. W.; and Dean, R. C. An Experimental Study of Surge in Multi-stage Compressor, ASME, *J. of Fluids Eng.*,(**1977**): 115-131.

[5] Baines, N. C. and Wallace F. J., Computer Aided Design of Mixed Flow Turbines for Turbocharges, *Journal of Engineering for Power, ASME*, 101(**1979**): 440-448

[6] Koçak, S., *Preliminary Design of Centrifugal Compressors*. ASME, Energy Week, Engineering Technology, Houston, **1996**, p308-313.

Copyright © 2013 by Modern Scientific Press Company, Florida, USA

[7] Rodgers, C., A Diffusion Factor Correlation for Multi-stage Impeller Stalling. ASME paper 78-GT-61, **1978**.

[8] Whitfield, A. and Baines, N. C., Design of Radial Turbomachines, New York, Longman Scientific Technical, **1990**.

[9] Koçak, S., Off-Design Operation of Impeller of the Centrifugal Compressor, Journal of Engineering Sciences, 10(2)(**2001**): 259-265.

[10] Aksel, M. H. and Eralp, O. C., *Gas Dynamics, New York*, Prentice Hall, **1994**.

[11] Öztürk, E., *Aerothermodynamics of Turbine Engines and Mechanics*, Istanbul, Birsen Yayınevi, **1997**.

[12] Brauembussche, R. A., Design and Optimization of Multi-stage Compressors, Thermodynamics and Fluid Mechanics of Turbomachinery, *NATO ASI Series E*, 97B(**1990**): 829-885.

[13] Koçak, S., Preliminary Design of Impeller of Multi-stage Compressors, Zonguldak Karaelmas University, *Journal of Technology*, 4 (1-2)(**2001**): 119-125.

Copyright © 2013 by Modern Scientific Press Company, Florida, USA

View publication stats